

## Internal friction peak in pure Al bicrystals with $\langle 100 \rangle$ tilt boundaries

W. B. Jiang,<sup>1</sup> P. Cui,<sup>1</sup> Q. P. Kong,<sup>1,\*</sup> Y. Shi,<sup>1</sup> and M. Winning<sup>2</sup>

<sup>1</sup>*Institute of Solid State Physics, Chinese Academy of Sciences, Hefei 230031, People's Republic of China*

<sup>2</sup>*Institut für Metallkunde und Metallphysik, RWTH Aachen, D-52056 Aachen, Germany*

(Received 1 July 2005; published 30 November 2005)

A substantial internal friction peak associated with grain boundary (GB) has been observed in pure aluminum bicrystals with  $\langle 100 \rangle$  tilt GBs, which is similar to that observed for  $\langle 112 \rangle$  tilt GBs in the previous work [Phys. Rev. B 71, 060101(R) (2005)]. The peak is suggested to be induced by GB sliding, but with different mechanisms in microscopic scale for different types of GBs by considering their difference in relaxation parameters. The relaxation parameters for low-angle GBs with a  $\langle 100 \rangle$  tilt axis are at the same level as those with a  $\langle 112 \rangle$  tilt axis, and can be interpreted by the glide and climb of dislocations composing the GB, but controlled by climb. The studied high-angle high  $\Sigma$  ( $\Sigma=29$ )  $\langle 100 \rangle$  tilt GB behaves similarly to high-angle general and high  $\Sigma$   $\langle 112 \rangle$  GBs; their mechanism is possibly associated with a local rearrangement of disordered atom groups. The studied low  $\Sigma$  ( $\Sigma=5$ )  $\langle 100 \rangle$  tilt GB exhibits a special behavior (i.e., high activation energy and low relaxation strength), which is attributed to its low free volume. The  $\langle 100 \rangle$  tilt GBs with angular deviations from exact  $\Sigma 5$  but within the near-CSL (coincidence site lattice) limit also exhibit some special behavior, but to a lesser extent.

DOI: [10.1103/PhysRevB.72.174118](https://doi.org/10.1103/PhysRevB.72.174118)

PACS number(s): 62.40.+i, 61.72.Mm, 61.72.Lk

### I. INTRODUCTION

The internal friction peak associated with the grain boundary (GB) in polycrystals was extensively investigated by Kê,<sup>1,2</sup> Benoit,<sup>3,4</sup> and others.<sup>5,6</sup> This peak has been used to study some GB related processes in polycrystalline materials.<sup>7-9</sup> But the data for polycrystals involve contributions of different types of GBs, from which the information of an individual GB cannot be evaluated.

There have been many investigations on the properties of bicrystals with different misorientation angles and different types of GBs.<sup>10-15</sup> However, the study on internal friction of bicrystals was seldom.<sup>16-18</sup>

Recently, we measured the internal friction of pure Al bicrystals with a series of  $\langle 112 \rangle$  tilt GBs, including low-angle, high-angle general and high  $\Sigma$  GBs.<sup>19</sup> The activation parameters of an internal friction peak were found to reveal a distinct change between low- and high-angle GBs, indicating different mechanisms. But in the work, no bicrystal with low  $\Sigma$  GB was included, due to the lack of low  $\Sigma$  GB for the  $\langle 112 \rangle$  tilt axis.

Since the GB properties depend not only on the misorientation angle but also on the tilt axis, the study of bicrystals with different tilt axes is necessary to get more information of the GB internal friction and the GB structure. Besides, a lot of works indicate that low  $\Sigma$  GBs often exhibit some special properties, such as high resistance to high-temperature GB sliding, fracture, and corrosion.<sup>10,11</sup> Hence, the present paper attempts to study the internal friction in pure Al bicrystals with a series of  $\langle 100 \rangle$  tilt GBs, including low angle, high angle, low  $\Sigma$ , and high  $\Sigma$  GBs.

### II. EXPERIMENTAL

The Al bicrystals used in this study were prepared by the Bridgman method. The total impurity content was 7.7 ppm,

the main impurity elements (in ppm) were as follows: P: 3.74; Si: 0.99; Ce: 0.99; Cu: 0.40; Fe: 0.36; La: 0.24; B: 0.18; As: 0.14; Th: 0.13; Ti: 0.12; V: 0.11. All the bicrystals were characterized to have a planar symmetric tilt GB with a  $\langle 100 \rangle$  tilt axis. The misorientation angles were 7.5°, 9.3°, 14.5°, 33.4°, 36.0° (close to  $\Sigma 5$ , 36.9°), 41.2°, and 43.1° (close to  $\Sigma 29$ , 43.6°).

The specimens were about 65 mm in length, 4 mm in width, and 2 mm in thickness. The planar boundary was parallel to the length and perpendicular to the width, located in the middle of the width. The specimen was clamped on the plane of the width at both ends. The length between clamps was about 50 mm, so the effective boundary area in the specimen was about  $50 \times 2$  mm<sup>2</sup>. During an internal friction measurement, the specimen was periodically twisted at the upper end, while the lower end was fixed.

The internal friction was measured using a forced vibration method at constant excitation strain amplitude  $1 \times 10^{-5}$  in an automatic inverted torsion pendulum. The internal friction  $Q^{-1}$  was determined by a direct measurement of the phase angle,  $\phi$ , by which the strain lags behind the stress. The measurements were taken in air at three frequencies (0.3, 1.0, and 3.1 Hz) with ascending or descending temperatures changing at the rate of 2 K/min.

The experimental procedures are similar to those in the previous work,<sup>19</sup> so that the data obtained in this study can be compared with Ref. 19.

### III. RESULTS

Figures 1(a)–1(c) show the internal friction vs temperature at 1 Hz in the pure Al bicrystals with misorientations 7.5°, 36.0° (close to  $\Sigma 5$ ), and 43.1° (close to  $\Sigma 29$ ), respectively. It can be seen that an obvious internal friction peak appears at medium temperature in the bicrystals, but disappears in the single crystals which were cut from the same

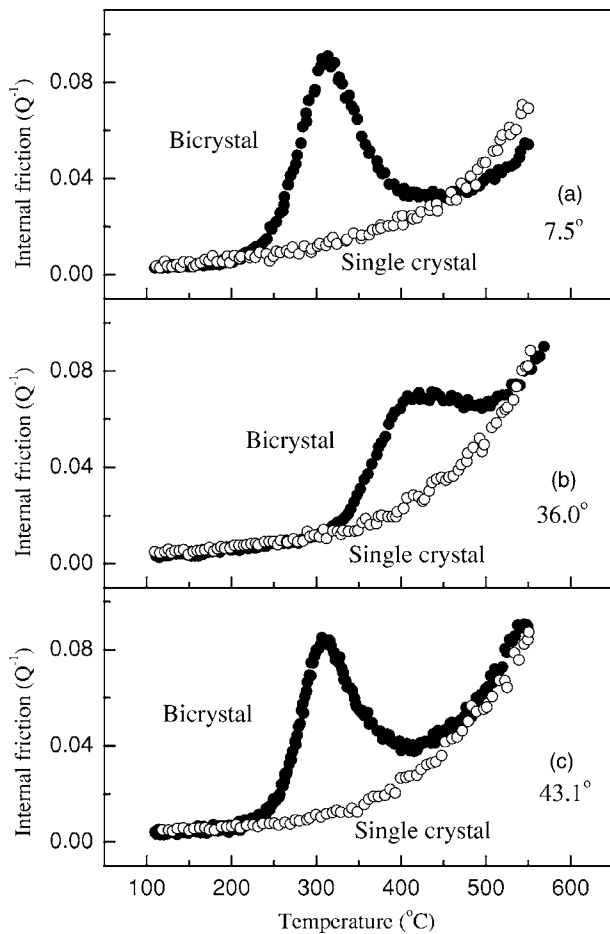


FIG. 1. The internal friction vs temperature in Al bicrystals with (a)  $7.5^\circ$ , (b)  $36.0^\circ$  (close to  $\Sigma 5$ ), and (c)  $43.1^\circ$  (close to  $\Sigma 29$ ), and the adjoining single crystals at 1 Hz.

grown product adjoining the bicrystals. It is evident that the observed peak should be associated with the GB. The peak is stable, appearing at both ascending and descending temperatures. It also appears in the other bicrystals listed above, and disappears in the corresponding single crystals.

Figure 2(a) shows an example for the internal friction measured at three different frequencies (0.3, 1.0, and 3.1 Hz) represented by the bicrystal with  $7.5^\circ$ . It can be seen that the peak shifts to higher temperature at higher frequency. Figure 2(b) shows the corresponding dynamic modulus (in arbitrary unit), which drops sharply around the internal friction peak temperature. In contrast, the modulus of the single crystals goes down slowly along a straight line, without the sharp drop (not shown here).

As is well known, the internal friction peak induced by an anelastic relaxation process occurs at the following condition:<sup>2,5</sup>

$$\omega\tau = \omega\tau_0 \exp(H/kT_p) = 1, \quad (1)$$

where  $\omega$  is the circular frequency ( $\omega = 2\pi f$ ,  $f$  is the measuring frequency),  $\tau$  is the relaxation time,  $\tau_0$  is the preexponential factor,  $H$  is the activation energy,  $k$  is the Boltzmann constant, and  $T_p$  is the absolute temperature of the peak.

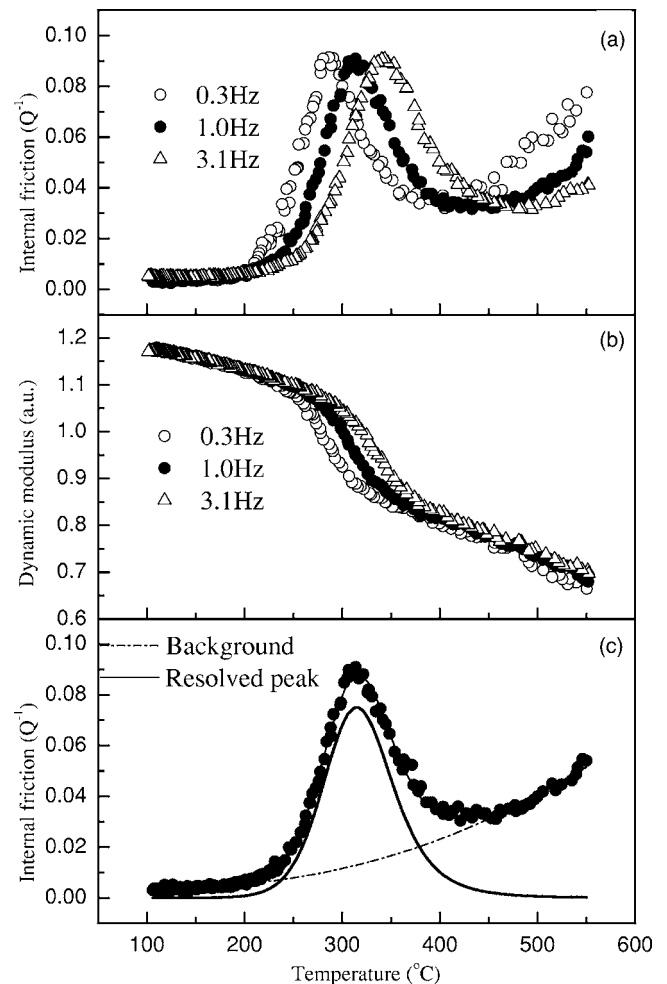


FIG. 2. (a) The internal friction and (b) dynamic modulus in the Al bicrystal with  $7.5^\circ$  measured at different frequencies, and (c) an example for resolving an experimental internal friction curve.

The peak was considered to be superimposed on a background  $Q_b^{-1}$  expressed by<sup>2,5</sup>

$$Q_b^{-1} = A_1 + A_2 \exp(-A_3/kT), \quad (2)$$

where  $A_1$ ,  $A_2$ , and  $A_3$  are constants. After subtracting the background by a fitting procedure<sup>20</sup> as used in Ref. 19, the net internal friction peak can be resolved from the experimental curve, as shown in Fig. 2(c).

The peak widths of the bicrystals are broader than that for a single relaxation time, the distribution parameters of relaxation time  $\beta$  are generally in the range of 1.0–0.25, which is similar to that for  $\langle 112 \rangle$  tilt GBs, but is smaller than that ( $\sim 3.5$ ) for ordinary polycrystals.

With the net peak height  $Q_{\max}^{-1}$  and the measured value of  $\beta$ , the relaxation strength can be determined according to the formula<sup>2,5</sup>

$$\Delta = \frac{Q_{\max}^{-1}}{f_2(0, \beta) - Q_{\max}^{-1}/2}, \quad (3)$$

where the values of parameter  $f_2(0, \beta)$  are obtained from Table 4.2 in Ref. 5.

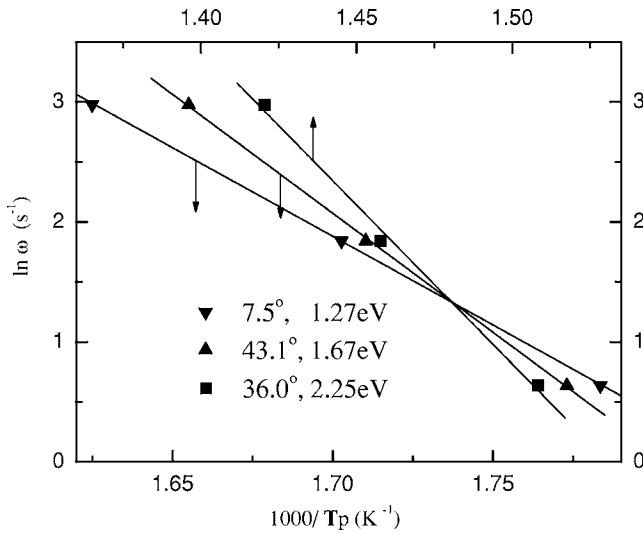


FIG. 3. Natural logarithm of the circular frequency  $\omega$  vs the reciprocal of the net peak temperature  $1/T_p$  for Al bicrystals with  $7.5^\circ$ ,  $36.0^\circ$ , and  $43.1^\circ$ .

With the net peak temperatures at different frequencies, the activation energy  $H$  and the preexponential factor  $\tau_0$  can be obtained based on Eq. (1). Figure 3 shows the Arrhenius plots (natural logarithm of circular frequency  $\omega$  vs the reciprocal of net peak temperature  $1/T_p$ ) for Al bicrystals with  $7.5^\circ$ ,  $36.0^\circ$ , and  $43.1^\circ$ . In Fig. 3, because the peak temperatures of  $36.0^\circ$  are much higher than others, two different scales of  $1/T$  at upper and lower abscissas are used for different bicrystals to condense the space of the figure.

The obtained values of  $H$ ,  $\tau_0$ ,  $Q_{\max}^{-1}$ , and  $\Delta$  for different misorientations are listed in Table I. The data of  $H$ ,  $\tau_0$  ( $\log_{10}\tau_0$ ), and  $\Delta$  vs the misorientation angle are plotted in Figs. 4(a)–4(c), respectively.

#### IV. DISCUSSION

During the measurement of internal friction, the planar GB in the bicrystals is subjected to a cyclic shear stress, which will induce a cyclic sliding (perhaps combined with rotation) of the GB. Thus the observed internal friction and

TABLE I. The activation energy  $H$ , the preexponential factor of relaxation time  $\tau_0$ , the internal friction peak height  $Q_{\max}^{-1}$ , and the relaxation strength  $\Delta$  for different misorientation angles  $\theta$  of planar symmetric  $\langle 100 \rangle$  tilt boundaries in pure Al bicrystals.

$\theta$	$H$ (eV) ( $\pm 0.05$ )	$\tau_0$ (s)	$Q_{\max}^{-1}$ ( $\pm 0.004$ )	$\Delta$ ( $\pm 0.02$ )
$7.5^\circ$	1.27	$1.9 \times 10^{-12 \pm 1}$	0.069	0.19
$9.3^\circ$	1.31	$1.5 \times 10^{-12 \pm 1}$	0.058	0.17
$14.5^\circ$	1.30	$1.6 \times 10^{-12 \pm 1}$	0.051	0.17
$33.4^\circ$	1.99	$4.8 \times 10^{-17 \pm 1}$	0.051	0.20
$36.0^\circ, \Sigma 5$	2.25	$3.6 \times 10^{-18 \pm 1}$	0.038	0.15
$41.2^\circ$	2.04	$1.4 \times 10^{-17 \pm 1}$	0.061	0.21
$43.1^\circ, \Sigma 29$	1.67	$6.2 \times 10^{-16 \pm 1}$	0.061	0.20

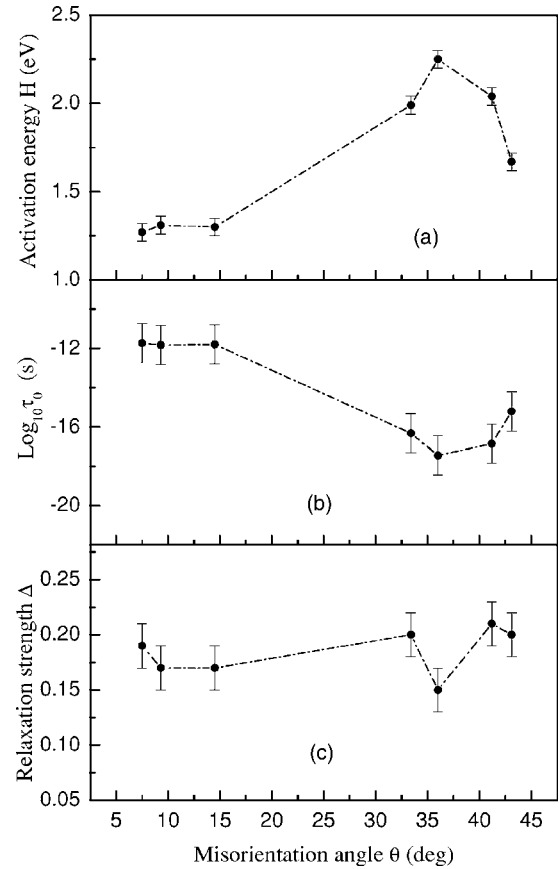


FIG. 4. (a) The activation energy  $H$ , (b) the logarithm of the preexponential factor of relaxation time  $\tau_0$ , and (c) the relaxation strength  $\Delta$  vs the misorientation angle.

modulus decrease can be attributed to the time-dependent GB sliding.

From Table I and Fig. 4, one can see that the relaxation parameters are different among different types of GBs. The origin and implications will be discussed jointly with the results obtained in the previous paper.<sup>19</sup>

##### A. On the relaxation parameters of low-angle GBs

The relaxation parameters of the  $\langle 100 \rangle$  tilt GBs with  $7.5^\circ$ ,  $9.3^\circ$ , and  $14.5^\circ$  are very similar to each other. Their activation energies  $H$  are about 1.3 eV, the preexponential factors of relaxation time  $\tau_0$  are of the order of  $10^{-12}$  s, and the relaxation strengths  $\Delta$  are in the range of 0.17–0.19. These parameters are on the same level within experimental error as those of low-angle  $\langle 112 \rangle$  tilt GBs<sup>19</sup> (for the latter, the values of  $H$  are about 1.4 eV;  $\tau_0$  is of the order of  $10^{-12}$ – $10^{-13}$  s; and  $\Delta$  is equal to 0.17–0.18). It indicates that the  $7.5^\circ$ ,  $9.3^\circ$ , and  $14.5^\circ$   $\langle 100 \rangle$  tilt GBs belong to a low-angle region, and that the low-angle  $\langle 100 \rangle$  and  $\langle 112 \rangle$  tilt GBs exhibit the same behavior.

In the tilt low-angle GBs, the dislocations can be considered as discrete. The spacing  $d$  between primary edge dislocations can be expressed by

$$d = b/\theta, \quad (4)$$

where  $\theta$  is the misorientation angle, and  $b$  is the magnitude of Burgers vector. The sliding of the low-angle GBs can be

accomplished by the glide and climb of dislocations composing the GB, but controlled by climb. The measured activation energy of internal friction is close to that of lattice diffusion (1.3 eV) in pure Al,<sup>21</sup> and is reasonable for the dislocation climb mechanism.

Winning<sup>15</sup> pointed out that the transition angle between low- and high-angle GBs depends on the critical spacing (or reversely, the critical density) of the dislocations composing the GB. From Eq. (4), we know that for 7.5°, 9.3°, and 14.5°,  $d=7.6b$ ,  $6.2b$ , and  $4.0b$ , respectively [the magnitude of Burgers vector  $b$  of  $1/2 \langle 110 \rangle$ -type dislocations in Al is 0.286 nm].<sup>15</sup> It implies that for the  $\langle 100 \rangle$  tilt GBs, when  $d \geq 4b$ , the GBs are in the low-angle region.

### B. On the relaxation parameters of high-angle general and high $\Sigma$ GBs

When  $\theta$  increases to the high-angle region, Eq. (4) is no longer valid, and the GBs cannot be described by regular arrays of primary dislocations. For  $\theta=43.1^\circ$  (close to  $\Sigma 29$ ), the data of  $H$  (1.67 eV),  $\tau_0$  ( $10^{-16}$  s), and  $\Delta$  (0.20), as given in Table I, are on the same level as those of general high-angle  $\langle 112 \rangle$  GBs and a high  $\Sigma$  ( $\Sigma=35$ )  $\langle 112 \rangle$  GB (Ref. 19) [for these  $\langle 112 \rangle$  GBs,  $H \approx 1.65$  eV,  $\tau_0 = 10^{-15} - 10^{-16}$  s, and  $\Delta = 0.17 - 0.26$ ]. It indicates that the behavior of the high  $\Sigma$  ( $\Sigma 29$ )  $\langle 100 \rangle$  GB is similar to that of high-angle general  $\langle 112 \rangle$  GBs and a high  $\Sigma$  ( $\Sigma=35$ )  $\langle 112 \rangle$  GB. This is in agreement with the criterion suggested by Palumbo and Aust<sup>11</sup> that when the value of  $\Sigma$  is equal to or larger than 29, the coincidence site lattice (CSL) GBs will lose their special properties. The structure of the high  $\Sigma$  GBs might be assumed to be similar to that of the general high-angle GBs.

In these GBs, the dislocations will no longer be discrete, but possibly degenerate to numerous disordered atom groups. The elementary process of GB sliding is possibly associated with a local rearrangement of disordered atom groups.<sup>2</sup>

The origin of the higher  $H$  ( $\sim 1.65$  eV) for these GBs is not clear at present. A possible explanation is the effect of impurity segregation. If we suppose that more impurities would segregate in these high-angle GBs owing to their stronger interaction with impurities, a higher  $H$  might occur.

### C. On the relaxation parameters of low $\Sigma$ and near-CSL GBs

Since the deviation angle of  $36.0^\circ$  from the exact  $\Sigma 5$  ( $36.9^\circ$ ) is less than  $1^\circ$ , we may call the  $36.0^\circ$  GB as a  $\Sigma 5$  GB for brevity. As will be seen below, the GBs with  $33.4^\circ$  and  $41.2^\circ$  can be called near-CSL (near  $\Sigma 5$ ) GBs.

The relaxation parameters of a  $36.0^\circ \langle 100 \rangle$  tilt GB ( $\Sigma 5$ ) are quite different from those of low-angle, high-angle general, and high  $\Sigma$  GBs. As shown in Table I, it has a high  $H$  (2.25 eV), a small  $\tau_0$  ( $10^{-18}$  s), and a low  $\Delta$  (0.15). Such a special behavior should originate from the fact that its microstructure is nearly the same as that of exact  $\Sigma 5$ , neglecting the secondary GB dislocations.

Figure 5 is a schematic illustration of a  $\Sigma 5 \langle 100 \rangle$  tilt GB in a face-centered-cubic lattice. One can see that the atoms

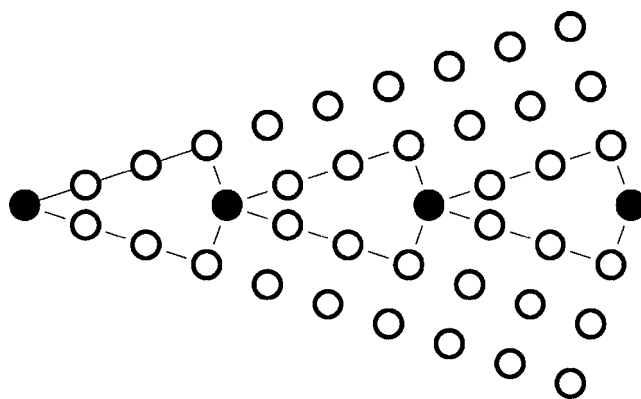


FIG. 5. Schematic illustration of  $\Sigma 5 \langle 100 \rangle$  tilt GB in a face-centered-cubic lattice.

composing the GB are closely packed and arranged in regular fashion. As pointed out by Sutton and Balluffi,<sup>10</sup> the efficiency of emission (absorption) of atoms (or vacancies) in such low  $\Sigma$  GBs is very low, so that an additional energy is needed to drive source (sink) action to accomplish the diffusion and the GB sliding. Besides, when an atom moves within the GB, the adjoining atoms should adjust their positions to keep the GB at low energy state; accordingly, a correlated motion should occur. Perhaps owing to the above-mentioned reasons, the high activation energy is observed. Since the atoms composing the low  $\Sigma$  GB are closely packed, the density of GB sliding units and hence the relaxation strength will be low.

It seems interesting to compare our internal friction data with those obtained by Li and Chou<sup>22</sup> in the diffusion of Cr along GB in Nb bicrystals. In their work, the activation energy was measured to be 1.68 eV for low-angle GBs ( $\leq 15.0^\circ$ ); about 1.8 eV for general high-angle GBs; and 2.29 eV for the  $\Sigma 5 \langle 001 \rangle$  GB. They attributed the high activation energy for the  $\Sigma 5$  GB to its low free volume. The results of GB diffusion in Ref. 22 are similar to those of internal friction in this study.

The activation parameters for  $33.4^\circ$  and  $41.2^\circ$  (both values of  $H$  are about 2.0 eV and  $\tau_0$  of the order of  $10^{-17}$  s) are near to those for  $36.0^\circ$  (see Table I). The reason may be originated from the fact that the angular deviations of both  $33.4^\circ$  and  $41.2^\circ$  from the exact  $\Sigma 5$  ( $36.9^\circ$ ) are within the near-CSL limit.

The criteria for the maximum angular deviations from exact CSL proposed by Brandon<sup>23</sup> and Palumbo and Aust<sup>15</sup> are, respectively,

$$\Delta \theta_1 = 15^\circ \Sigma^{-1/2}, \quad (5)$$

$$\Delta \theta_2 = 15^\circ \Sigma^{-5/6}. \quad (6)$$

For  $\Sigma 5$ , we have  $\Delta \theta_1 = 6.7^\circ$  and  $\Delta \theta_2 = 5.5^\circ$  according to Eqs. (5) and (6), respectively. One can see that whatever criterion is used, the deviations of both  $33.4^\circ$  and  $41.2^\circ$  from  $36.9^\circ$  (i.e.,  $3.5^\circ$  and  $4.3^\circ$ ) are within the limit, and hence they can keep some “special” properties, but to a lesser extent. Their GB structure can still be described by Fig. 5, but accommo-



dated with localized networks of secondary GB dislocations (SGBDs).<sup>10</sup>

In the near-CSL GBs, the efficiency of the source (sink) is still limited, but the atom diffusion can be accomplished via the climb of SGBDs.<sup>10</sup> Hence the activation parameters are near to those of CSL GBs.

#### D. On the relaxation strength and GB sliding displacement

The maximum relaxation strengths  $\Delta$  for the bicrystals with  $\langle 100 \rangle$  and  $\langle 112 \rangle$  tilt GBs are 0.21 (Table I) and 0.26 (Ref. 19), respectively. They are lower than that (about 0.5) for Al polycrystals (with purity of 99.99% or 99.999%).<sup>2</sup> It can be understood by the fact that the GB area in the unit volume of the bicrystals is much lower than that of ordinary polycrystals (with grain sizes of 0.2–0.8 mm).

If we adopt the viscous sliding model,<sup>2</sup> the GB sliding displacement in the bicrystals can be estimated from the relaxation strength and the specimen dimension, as we did in Ref. 19. In the internal friction measurement, the strain amplitude ( $\varepsilon=10^{-5}$ ) includes the elastic strain  $\varepsilon_0$  and the anelastic strain  $\varepsilon_a$  (which is caused by GB sliding). Based on the dimension of the specimen (the width  $s=4\text{ mm}=4 \times 10^6\text{ nm}$ ), the total displacement along the planes parallel to GB in the whole specimen is  $x=\varepsilon s=40\text{ nm}$ . In order to separate  $\varepsilon_a$  from the total strain, we use the following equation:<sup>5,19</sup>

$$\Delta = \frac{M_U - M_R}{M_R} = \frac{\varepsilon_a}{\varepsilon_0}, \quad (7)$$

where  $M_U$  and  $M_R$  are unrelaxed and relaxed moduli, respectively. From Eq. (7), we have

$$\varepsilon_a = (\varepsilon_0 + \varepsilon_a) \frac{\Delta}{1 + \Delta} = 10^{-5} \frac{\Delta}{1 + \Delta} = \frac{x_a}{s}, \quad (8)$$

where  $x_a(=\varepsilon_a s)$  is the GB sliding displacement. Using  $s=4 \times 10^6\text{ nm}$ , and substituting the lowest value  $\Delta=0.15$  and the highest value  $\Delta=0.21$  (Table I) into Eq. (8), we obtain  $x_a=5.2\text{ nm}$  and  $6.9\text{ nm}$ , respectively. Thus the sliding displacements of the  $\langle 100 \rangle$  GBs are in the range of 5.2–6.9 nm, which are similar to those (4.6–8.2 nm) for  $\langle 112 \rangle$  tilt GBs in bicrystals as estimated in the previous paper.<sup>19</sup>

The sliding displacement of GBs in internal friction of ordinary polycrystals was estimated by Raj and Ashby<sup>24</sup> assuming that the GBs have a sinusoidal shape. The average value estimated is about 5 nm, which is of the same order as those in the bicrystals.

The detailed mechanism of the GB internal friction peak is to be further studied for bicrystals and polycrystals. For the bicrystals, the mechanism of low-angle GBs is relatively clear, while that of high-angle GBs needs more effort.

#### V. SUMMARY

(1) A substantial internal friction peak associated with the grain boundary (GB) has been observed in pure aluminum bicrystals with  $\langle 100 \rangle$  tilt GBs which is similar to that observed for  $\langle 112 \rangle$  tilt GBs in the previous work. The peak is suggested to be induced by GB sliding, but with different mechanisms in microscopic scale for different types of GBs by considering their difference in relaxation parameters.

(2) The relaxation parameters for low-angle GBs with  $\langle 100 \rangle$  tilt axis are at the same level as those with  $\langle 112 \rangle$  tilt axis. They are interpreted by the glide and climb of dislocations composing the GB, but controlled by the climb.

(3) The peak for the studied high  $\Sigma$  tilt GBs [including a  $\Sigma 29$   $\langle 100 \rangle$  tilt GB and a  $\Sigma 35$   $\langle 112 \rangle$  tilt GB] behaves similarly to that of high-angle general tilt GBs. This is in agreement with the criterion suggested by Palumbo and Aust that when  $\Sigma \geq 29$ , the CSL GBs will lose their special properties. The mechanism of the peak for high-angle general and high  $\Sigma$  GBs is possibly associated with a local rearrangement of disordered atom groups.

(4) The peak for the studied low  $\Sigma$  ( $\Sigma=5$ )  $\langle 100 \rangle$  tilt GB exhibits a special behavior (i.e., high activation energy and low relaxation strength), which is attributed to its low free volume. The  $\langle 100 \rangle$  tilt GBs with angular deviations from exact  $\Sigma 5$  but within the near-CSL limit also exhibit some special behavior, but to a lesser extent.

(5) The GB sliding displacement in an internal friction measurement has been estimated from the relaxation strength and specimen dimension for the bicrystals. The estimated values for  $\langle 100 \rangle$  tilt GBs are in the range of (5.2–6.9 nm), which are comparable with those (4.6–8.2 nm) estimated for  $\langle 112 \rangle$  tilt GBs, and of the same order as that ( $\sim 5\text{ nm}$ ) estimated by Raj and Ashby in ordinary polycrystals.

#### ACKNOWLEDGMENTS

This work has been supported by the National Natural Science Foundation of China (NSFC) under Grant No. 10274085 and the German Research Foundation (DFG) through Contract No. Wi 1917/1. We are thankful to Professor G. Gottstein and Professor Q. F. Fang for helpful discussions.

\*Author to whom correspondence should be addressed. FAX: +86-551-5591434. Email address: qpkong@issp.ac.cn

<sup>1</sup>T. S. Kê, Phys. Rev. **71**, 533 (1947).

<sup>2</sup>T. S. Kê, Metall. Mater. Trans. A **30**, 2267 (1999).

<sup>3</sup>W. Benoit, Mater. Sci. Forum **366-368**, 291 (2001); **366-368**, 306 (2001).

<sup>4</sup>W. Benoit, Mater. Sci. Eng., A **370**, 12 (2004).

<sup>5</sup>A. S. Nowick and B. S. Berry, *Anelastic Relaxation in Crystalline Solids* (Academic Press, New York, 1972).

<sup>6</sup>H. Gleiter and B. Chalmers, *High Angle Grain Boundaries* (Pergamon Press, Oxford, 1972).

<sup>7</sup>T. S. Kê and P. Cui, Scr. Metall. Mater. **26**, 1487 (1995).

<sup>8</sup>Q. P. Kong, B. Cai, and G. Gottstein, J. Mater. Sci. **36**, 5429 (2001).

- <sup>9</sup>Y. Shi, B. Cai, Q. P. Kong, P. Cui, and G. Gottstein, *J. Mater. Sci.* **38**, 1895 (2003).
- <sup>10</sup>A. P. Sutton and R. W. Balluffi, *Interfaces in Crystalline Materials* (Oxford University Press, Oxford, 1995).
- <sup>11</sup>G. Palumbo and K. T. Aust, in *Materials Interface*, edited by D. Wolf and S. Yip (Chapman and Hall, London, 1992), p. 190.
- <sup>12</sup>M. Winning, G. Gottstein, and L. S. Shvindlerman, *Acta Mater.* **49**, 211 (2001).
- <sup>13</sup>M. Winning, G. Gottstein, and L. S. Shvindlerman, *Acta Mater.* **50**, 353 (2002).
- <sup>14</sup>M. Winning, *Acta Mater.* **51**, 6465 (2003).
- <sup>15</sup>M. Winning and A. D. Rollett, *Acta Mater.* **53**, 2901 (2005).
- <sup>16</sup>M. Kato and T. Mori, *Philos. Mag. A* **68**, 939 (1993).
- <sup>17</sup>L. X. Yuan and T. S. Kê, *Phys. Status Solidi A* **154**, 573 (1996).
- <sup>18</sup>X. G. Guan and T. S. Kê, *J. Alloys Compd.* **211/212**, 480 (1994).
- <sup>19</sup>Y. Shi, P. Cui, Q. P. Kong, W. B. Jiang, and M. Winning, *Phys. Rev. B* **71**, 060101(R) (2005).
- <sup>20</sup>Q. F. Fang, *Acta Metall. Sin.* **32**, 565 (1996).
- <sup>21</sup>J. Philibert, *Diffusion et Transport de Matière dans les Solides* (Les Editions de Physique, Les Ulis Cedex, France, 1985).
- <sup>22</sup>X. M. Li and Y. T. Chou, *Acta Mater.* **44**, 3535 (1996).
- <sup>23</sup>D. G. Brandon, *Acta Metall.* **14**, 1479 (1966).
- <sup>24</sup>R. Raj and M. F. Ashby, *Metall. Trans.* **2**, 1113 (1971).